Solid-state synthesis and dielectric properties of nanocomposites containing poly (3,4-ethylenedioxythiophene) /graphene nanoplatelets

Chitragara Basavaraja, Ju Yeon Park, Do Sung Huh

Abstract— **New conducting polymer nanocomposites of poly(3,4-ethylenedioxythiophene) (PEDOT) were prepared by simple solid-state heating polymerization of 2,5-dibromo-3,4-ethylenedioxythiophene (EDOT) with different concentrations (weight percentage) of graphene nanoplatelets (GNPs). The prepared PEDOT/GNP nanocomposites were characterized through Fourier transform infrared (FTIR) and UV–vis spectroscopy, and their surface morphology was analyzed through scanning electron and transmission electron microscopy. The FTIR and UV–vis spectra revealed strong interaction between the PEDOT matrix and GNPs. The frequency-dependent AC electrical conductivity of the prepared nanocomposites was obtained at room temperature within the frequency range of 100 Hz to 2.3 × 10^6 Hz. The conductivity of the composites significantly increased with increasing frequency compared with that of PEDOT and GNPs.**

Index Terms—**Dielectric properties, Graphene nanoplatelets, Nanomaterials, Polymer composites, PEDOT**

I. INTRODUCTION

Lightweight, inexpensive, flexible, and environment-friendly energy storage devices are in high demand for a number of applications, including new types of portable electronics, propulsion of all-electric or hybrid vehicles, and management of intermittent renewable energy sources [1]. As a result of these needs, studies have been conducted to develop thin flexible lithium-ion batteries [2] and novel current collectors for such devices [3]. Another approach to obtain flexible energy storage involves the utilization of conducting polymers, which provide promising aspects in terms of easy manufacturing, inexpensive raw materials, and environment friendliness [4]. Since the discovery of the conductive properties of doped polyacetylene, various polymers with conductive properties have been presented [5].

Conducting polymers (CPs) that have been investigated include poly(acetylene), polypyrrole, poly(phenylene vinylene), poly(pyrrole), poly(thiophenes), and their various derivatives [6].

Chitragara Basavaraja, Department of Chemistry Nano Science and Engineering, Institute of Nano manufacturing, Inje University, Kimhae, Kyungnam 621-749, South Korea, Mobile No.+8210-6496-6589

Ju Yeon Park, Department of Chemistry Nano Science and Engineering, Institute of Nano manufacturing, Inje University, Kimhae, Kyungnam 621-749, South Korea, Mobile No.8210-6616-8-33.

Do Sung Huh, Department of Chemistry Nano Science and Engineering, Institute of Nano manufacturing, Inje University, Kimhae, Kyungnam 621-749, South Korea, Mobile No. 8210-9303-9265.

Poly (3,4-ethylenedioxythiophene) (PEDOT) has gained significant research attention because of its superior qualities over other polymers; such properties include high stability, enhanced light transmission, processability, and simple production [7]. PEDOT is a superior material and an effective CP because of its low band gap, excellent environmental stability, high electrical conductivity, and transparency in thin oxidized films. PEDOT has been extensively studied since it was first synthesized in 1989 [8]. This polymer can be used in solid electrolytic capacitors, anti-electrostatic agents, transparent electrodes in light-emitting diodes, and under-layers for metallization of printed circuit boards. High light transmissivity is an important characteristic of PEDOT, which is light blue in the oxidized state and very dark blue in the reduced state. Doping of PEDOT can generate variable band gaps that range from 1.4 eV to 2.5 eV, resulting in a wide array of attainable colors[9], [10]. This high light transmissivity has impelled the industrial applications of PEDOT on anti-static coatings in photographic films, solar cells, and smart windows.

Given that pure PEDOT bulk material is insoluble and infusible, a considerable number of studies have focused on developing a solution-processable formulation. Although electrochemical polymerization is widely used to fabricate conductive polymer thin films, the required conducting substrate in which the polymer is formed may restrict its applications [11]. An alternative approach is to use PEDOT as conducting composite or as a mixture with conventional polymers. In this process, materials with superior functional properties are incorporated into CPs to improve the polymer properties, resulting in reduced quantity of the required material and improved properties of the composite materials[12] – [15]. The presence of heterogeneous medium comprising a semi-crystalline polymer matrix and inorganic materials imparts a condition in which dipoles are inherently created and remain trapped in the multi-phase microstructure of the composite. The dipoles produced from spatial distribution of cations or anions exhibit relaxation behavior and control the dielectric and conductive properties of a nanocomposite system [16].

Graphene is one of the most promising carbon-based nanofillers, following fullerene and carbon nanotubes, used for polymer nanocomposites. This carbon features large specific surface areas [17], excellent electrical conductivity [18], high charge carrier mobility [19], and easy coagulation in aqueous media and polar solvents. Producing graphene is inexpensive because it can be easily oxidized or reduced. Graphene also exhibits high electrical conductivity, high thermal conductivity, extraordinary elasticity, and stiffness [20]. Addition of graphene to polymers can enhance the

mechanical, electrical, and thermal properties of the resulting nanocomposites [21], [22]. Graphene-based polymer composites with high electrical and thermal conductivity are preferred in several applications, such as electronic devices, electromagnetic shielding, and thermal management [23] – [25].

Graphene nanoplatelets (GNPs) are multilayer particles that consist of 10 to 30 sheets of graphene and exhibit preserved single-layer properties [26], [27]. GNPs are widely used because they are inexpensive and easier to produce than single-layer graphene or carbon nanotubes [28]. GNPs can be easily dispersed, whereas a single-layer graphene can curl during dispersion. GNPs exhibit a low relative surface area and a potential for strong interfacial bonding with the matrix because of their high surface energy. This high surface energy is attributed to the high surface area intrinsic to the geometry of GNPs. Although polymer/graphene can be fabricated using currently available methods, a simple and efficient synthesis technique must be developed.

In this study, PEDOT/graphene nanocomposites were prepared by in situ solid-state heating polymerization of 2,5-dibromo-3,4-ethylenedioxythiophene (EDOT). During polymerization, GNP concentration varied from 10, 20, and 30 wt% and EDOT concentration was fixed. The synthesized nanocomposites were characterized through Fourier transform infrared (FTIR) and UV–vis spectroscopy. The morphology of the nanocomposites was investigated through scanning electron microscopy (SEM) and transmission electron microscopy (TEM), and diffraction patterns were evaluated by X-ray diffraction (XRD) analysis. The AC electrical conductivity of the nanocomposites was measured within the range of 100 Hz to 2.3 × 10^6 Hz at room temperature.

II. EXPERIMENTAL

Materials

EDOT (99%) was purchased from Sigma–Aldrich, and GNP KNG-150 was obtained from Xiamen Kano Graphite Technology Co. Ltd., Xiamen, China. N-Methyl-2-pyrrolidinone (NMP) was obtained from Junsei Chemical Co. Double-distilled water was used throughout the experiment.

Preparation of PEDOT and PEDOT/GNP nanocomposites

PEDOT was prepared in situ through simple solid-state polymerization of EDOT. A known amount of EDOT was added to the chloroform containing GNPs, and the monomer was adsorbed on the GNP surface through sonication. The mixture was placed in a vacuum oven at 60 °C to evaporate chloroform, and the residue was stored in the oven under similar conditions for 24 h [29]. The synthesis scheme of the composites is shown in Fig.1. Addition and sonication of chloroform dispersion containing GNPs and EDOT formed a complex structure in the initial stages. During sonication, the EDOT monomer attached on the surface of the scalar- or flake-like structure of GNPs and then formed a complex structure. When placed in a vacuum oven at 60 °C to evaporate chloroform, EDOT undergoes polymerization to form PEDOT/GNP nanocomposites. For comparison, pure PEDOT was synthesized using similar method but without addition of GNPs in the reaction medium.

To investigate the effect of GNPs on the conductivity of the composites, we varied the concentration of GNPs (wt %) from 10%, 20%, and 30% during preparation and designated the corresponding PEDOT/GNP polymer nanocomposites as PEDOT/GNP–10, PEDOT/GNP–20, and PEDOT/GNP–30, respectively.

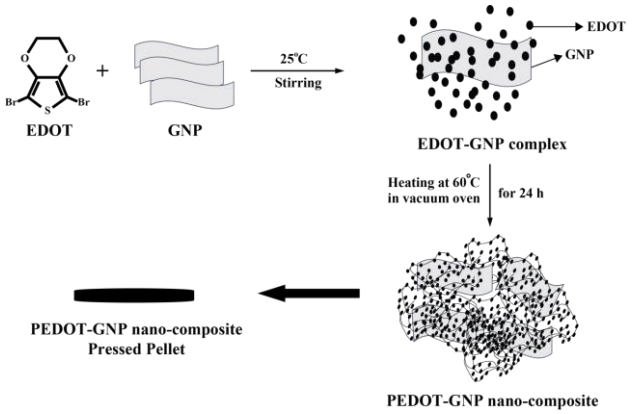

Fig. 1. Schematics of the preparation of PEDOT/GNP nanocomposites.

Characterization and property evaluation of PEDOT and PEDOT/GNP nanocomposites

Infrared spectra of the polymer and nanocomposite samples pelletized with KBr were determined using an FTIR spectrometer (Perkin–Elmer Model 1600) at a resolution of 2 cm^{-1} within the range of 4,000 cm^{-1} to 400 cm^{-1}. XRD patterns were obtained with a Philips diffractometer (PW 1710) with Cu Kα (λ = 1.5406 Å) radiation. Diffractograms were recorded in terms of 2θ within the range of 5° to 0° at a scanning rate of 2° per min. Powder morphology was investigated through SEM (Philips XL-30 ESEM) and TEM (JOEL, JEM-2010). Meanwhile, the powder morphology of the synthesized composites was investigated through SEM (COXEM-CX100s) TEM (JEM-2000, JEOL, Japan). The atomic and weight percentages of the elements in the polymer composites were analyzed using an energy-dispersive X-ray (EDX) analyzer equipped to the SEM. UV–vis spectra were determined using a Shimadzu UV–vis/NIR spectrophotometer (UV-3101PC) with NMP. AC conductivity was determined with a Hewlett–Packard 4284A impedance analyzer. Fine copper wires were used as connecting wires, and silver paste was applied as coating material. Capacitance (C) and dissipation factors (D) were measured at various frequencies. AC conductivity $\sigma(\omega)$ and real parts of dielectric permittivity (ε') were calculated using the following relationship: $G = D\omega C$, $\sigma = Gd/A$, and $\varepsilon' = Cd/A$, where G is the conductance, A is the electrode area, and d is the sample thickness.

III. RESULTS AND DISCUSSION

Fig.2 shows the FTIR transmittance spectra of PEDOT, GNPs, PEDOT/GNP–10, PEDOT/GNP–20, and PEDOT/GNP–30 within the range of 500–4000 cm^{-1}. Table I presents the approximate peak assignment transmission bands for PEDOT, GNPs, PEDOT/GNP–10, PEDOT/GNP–20, and PEDOT/GNP–3. The approximate transition peaks at 1515 and 1315 cm^{-1} are assigned to the asymmetric stretching mode of C=C and the inter-ring stretching mode of C–C [26],

respectively. The peaks at approximately 1230, 1135, and 1085 cm^{-1} are attributed to the C–O–C bending vibration in ethylenedioxy [29], [30]. The approximate transition peaks at 686, 824, 915, and 968 cm^{-1} are the characteristic bands of the stretching vibrations of the C–S–C bond in the thiophene ring. The GNP peaks located at 1666, 3047, and 3425 cm^{-1} correspond to O–H, C–H, and C=C, respectively. The wide absorption band at 1566 and 1635 cm^{-1} is attributed to the stretching vibration of –C=C– [31]. The FTIR transmittance spectra of the PEDOT/GNP–10, PEDOT/GNP–20, and PEDOT/GNP–30 nanocomposites were similar to that of PEDOT. However, some bands related to PEDOT were modified with the incorporation of GPNPs. The transmittance peaks of the PEDOT/GNP nanocomposite shifted by a factor of 8–10 cm^{-1} in the peaks related to the stretching vibrations of the C–C, C = C, C–O–C, and C–S–C bonds. The labeled transmission peaks shown in Fig.2 indicated the strong interaction between PEDOT and GNPs in the PEDOT/GNP nanocomposites.

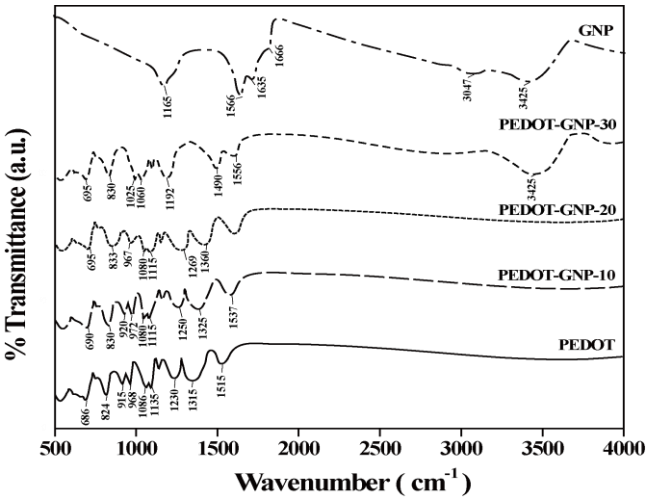

Figure 2: FTIR spectra of GNPs, PEDOT, PEDOT/GNP–10, PEDOT/GNP–20, and PEDOT/GNP–30.

Fig.3 shows the UV–vis absorption spectra of PEDOT, GNPs, and PEDOT/GNP nanocomposites obtained with 3 mg/ml NMP solvent. The UV–vis absorption spectrum of pure PEDOT showed absorption bands at 325, 417, 465, and 508 nm, which can be attributed to the absorption peaks arising from the conjugated segments with different conjugation lengths; these bands are assigned to the $\pi \rightarrow \pi^*$ transition of the thiophene ring. The absorption band at 785 nm is assigned to the polaron and/or bipolaron band, which indicates strong interaction among PEDOTs [29], [30]. The spectra of GNPs indicated that the absorption band at 340 nm is attributed to the $\pi \rightarrow \pi^*$ of graphene [31]. The absorption spectra of the PEDOT/GNP nanocomposites show all the bands related to PEDOT and GNPs. The absorption spectra of PEDOT/GNP–10 and PEDOT/GNP–20 show similar spectra to that of PEDOT with broadening of the absorption band at 325 nm; the broadened band is attributed to the presence of low concentration of GNPs in the composites. Furthermore, a small increase in the concentration of GNPs causes the broadening of the absorption band at 343 nm. The bands related to PEDOT present red shift in the absorption bands in PEDOT/GNP–30. Except for a slight broadening of some absorption bands, the incorporation/doping of GNPs in PEDOT does not cause any significant modifications in the spectra of PEDOT/GNPs.

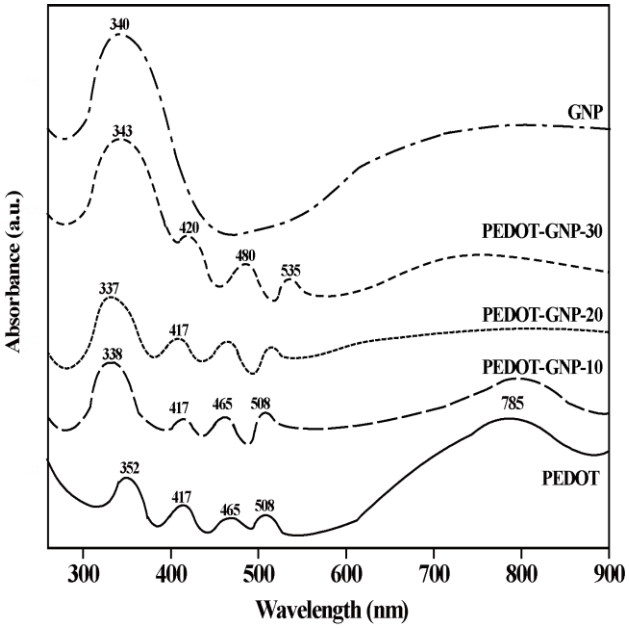

Fig. 3. UV-vis spectra of GNPs, PEDOT, PEDOT/GNP–10, PEDOT/GNP–20, and PEDOT/GNP–30.

The surface morphology of PEDOT and PEDOT/GNP nanocomposites were studied through SEM. Fig.4 shows the SEM images of PEDOT, PEDOT/GNP–10, PEDOT/GNP–20, and PEDOT/GNP–30 at 10 µm magnification. The surface image of PEDOT demonstrated granular structures or spherical particles, which are not clearly visible. The SEM image of PEDOT/GNP–10 showed some solid structures along the granular-like structures of PEDOT when GNPs were incorporated. The SEM image of PEDOT/GNP–20 showed lump-like structures with a small increase in GNP concentration, whereas the SEM image of PEDOT/GNP–30 showed some scalar- or flake-like structures, over which some spherical-like particles appeared to be attached to the surface, with further increase in GNP concentration. The scalar- or flake-like structures represent GNPs, and the attached spherical-like particles correspond to the PEDOT polymer.

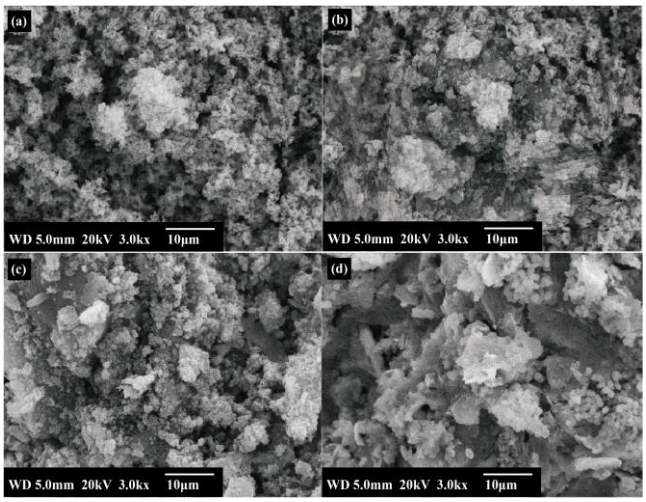

Fig. 4. SEM images of PEDOT, PEDOT/GNP–10, PEDOT/GNP–20, and PEDOT/GNP–30.

TABLE 1. Atomic and weight percentage data obtained from EDS spectra for PEDOT, GNPs, PEDOT/GNP –10, PEDOT/GNP–20, and PEDOT/GNP–30.

Element	Atomic %			Weight %		
	C	O	S	C	O	S
PEDOT	36.3	64.1	28.7	31	58.6	24.4
PEDOT/GNP –10	21	50.2	14.8	14.4	49.0	27.0
PEDOT/GNP–20	40.8	41.4	7.9	29.9	41.7	13.8
PEDOT/GNP–30	49.5	31.4	7.0	37.4	36.8	16

Fig. 5 shows the TEM images of PEDOT, PEDOT/GNP–10, PEDOT/GNP–20, and PEDOT/GNP–30 at 100 nm. Fig. 5(a) shows the sphere-like particles of PEDOT, with diameters of approximately 40–60 nm. The spherical particles attached to one another and resembled clouds with interconnected networks. With the incorporation of GNPs in PEDOT, the SEM image of PEDOT/GNP–10 presented a cloud-like structure with gray and black colored area, in which a scalar- or flake-like structure of GNPs is attached on the surface of the polymer structures of PEDOT. With increase in GNP concentration in the nanocomposites, a large amount of PEDOT polymer structures attached to the scalar- or flake-like structure of GNPs, resulting in enlarged black colored area of the image. This finding was demonstrated in the images of the PEDOT/GNP–20 and PEDOT/GNP–30 nanocomposites in Figs. 5(c) and 5(d), respectively.

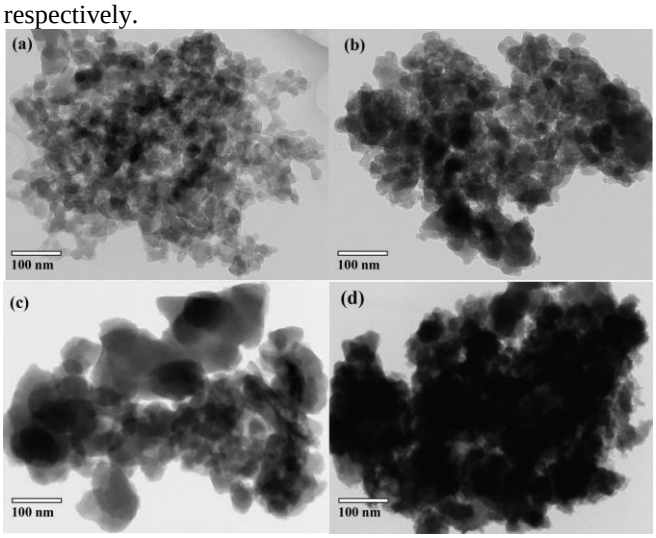

Fig. 5. TEM images of PEDOT, PEDOT/GNP–10, PEDOT/GNP–20, and PEDOT/GNP–30.

Table 1 shows the atomic and weight percentage data for C, S, and O obtained from the EDS spectra of PEDOT, PEDOT/GNP–10, PEDOT/GNP–20, and PEDOT/GNP–30. According to Table I, C, S, and O exist in PEDOT. A high percentage of C was observed in the PEDOT/GNP samples, which could be attributed to the increase in GNP concentration in PEDOT/GNP. By contrast, the percentage of O and S decreased, which is due to the partial oxidation of GNP and PEDOT chains during the formation of PEDOT/GNP, respectively. The reaction scheme of Fig.1 suggests the possible involvement of S in the formation of PEDOT/GNPs.

Fig.6 shows the XRD patterns of PEDOT and PEDOT/GNP nanocomposites. The XRD patterns of PEDOT showed that the diffraction peak located at 2θ = 25° can be referred to the inter-chain planar ring stacking distance [31], [32]. The XRD patterns of GNPs demonstrated three other peaks at 2θ values of 43.5°, 45.5°, and 54.3°, which correspond to the (100), (101), and (004) planes, respectively. The most intense peak was observed at 26.5°, which corresponds to the (002) plane of hexagonal graphite, with a d-spacing of 0.34 nm. The XRD peaks of GNPs were similar to the sample indexed in JCPDS No. 00-012-0212 and correspond to a few layered structures present in the sample [33], [34]. At low GNP concentrations, the PEDOT/GNP–10 nanocomposite demonstrated nearly a broad diffraction peak at 2θ between 25° and 27° and three approximately broad bands at 2θ values of 43.5°, 45.5°, and 54.3°. As the concentration of GNPs increased, the diffraction patterns of PEDOT diminished and definite and strong diffraction peaks related to GNPs were exhibited by the PEDOT/GNP–20 and PEDOT/GNP–30 nanocomposites. As the concentration of GNPs further increased, the diffraction peaks related to GNPs became predominant and the diffraction peaks related to diminished. The diffraction patterns in Figure 6 revealed the crystalline nature of the PEDOT/GNP nanocomposites.

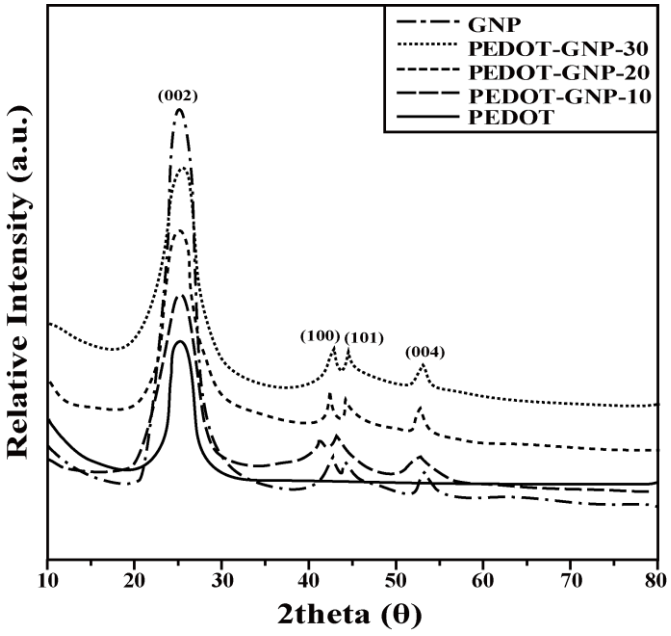

Fig. 6. X-ray diffraction patterns of GNPs, PEDOT, PEDOT/GNP –10, PEDOT/GNP–20, and PEDOT/GNP–30.

Fig.7 shows the frequency-dependent AC electrical conductivity of PEDOT, GNPs, and PEG nanocomposites at room temperature within the frequency range of 100 Hz to 2.3 × 10^{6} Hz. Generally, AC electrical conductivity increased with increasing frequency in all samples. Meanwhile, AC electrical conductivity was higher than that in pure PEDOT and increased with increasing GNP concentration in the PEDOT/GNP nanocomposites. The AC electrical conductivities at 100 Hz for PEDOT, GNP, PEDOT/GNP–10, PEDOT/GNP–20, and PEDOT/GNP–30

were 2.15, 3.98, 9.65, 6.16, and 7.89 S/cm, respectively. Similarly, the AC electrical conductivities at 2.3×10^6 Hz for PEDOT, GNPs, PEDOT/GNP–10, PEDOT/GNP–20, and PEDOT/GNP–30 were 8.35, 9.68, 21.56, 17.95, 19.7 S/cm, respectively. These findings indicate that AC electrical conductivity of GNPs exhibited higher conductivities than that of the PEDOT polymer, and that of the PEDOT/GNP composites was higher than that of pure PEDOT but lower than that of GNPs. The high electrical conductivity is mainly attributed to the crystalline nature of GNPs, whereas the low electrical conductivity is due to the amorphous nature of PEDOT. The obtained electrical conductivity of PEDOT/GNPs was higher than that of pure PEDOT polymer.

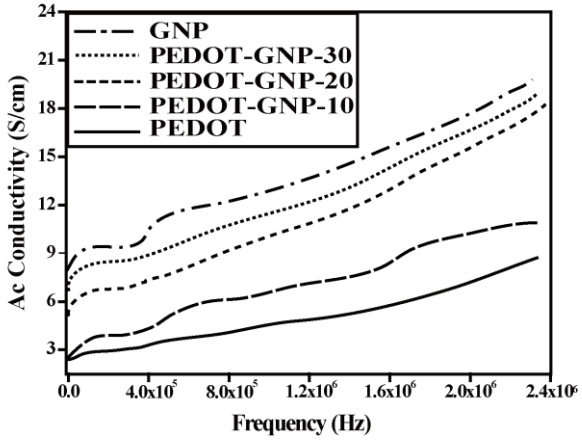

Fig. 7. Frequency-dependent AC electrical conductivity of PEDOT, GNPs, PEDOT/GNP–10, PEDOT/GNP–20, and PEDOT/GNP–30 at room temperature within the frequency range of 3.5×10^4 Hz to 2.3×10^6 Hz.

Fig.7 shows that the increase in the conductivity values of the PEDOT/GNP nanocomposites is mainly attributed to the presence of highly conducting GNPs, which possibly enhance the conductivity, and to the intermixing of PEDOT and GNPs during synthesis, as revealed by surface morphology data. In addition, the presence of carboxyl (–C=O) group in GNPs may facilitate the interaction between PEDOT and GNPs in the nanocomposites. As shown in Figure 1, the formation of a complex structure during synthesis of PEDOT/GNP nanocomposites was induced by interactions between the EDOT monomer and the dispersed GNPs. Moreover, surface morphology and diffraction studies indicated that the increase in conductivity may be attributed to the increase in orderliness in the PEDOT/GNP composites; the increased orderliness enhances the compactness and molecular orientations of the composites, thereby increasing the conductivity.

Figs. 8(a) and (b) present the frequency-dependent dielectric constants and dielectric losses, respectively, of PEDOT, GNPs, and PEDOT/GNP nanocomposites within the frequency range of 100 Hz to 2.3×10^6 Hz. Both the dependent dielectric constants and dielectric losses of GNPs exhibited higher conductivities compared with those of the PEDOT polymer. The values of the PEDOT/GNP composites were higher than those of pure PEDOT but lower than those of GNPs. Figs. 8(a) and (b) show the decrease in dielectric constants and dielectric losses with increasing frequency. The dielectric behavior value of the PEDOT/GNP nanocomposites was high under low frequencies and low under high frequencies, and this trend is opposite to that of the conductivity behavior of the PEDOT/GNP nanocomposites. As GNP concentration increased in the polymer composite, the orderliness increased and thus packing density also increased. The presence of increased orderliness at the interface between the polymer and oxide led to maximum space charge polarization and thus contributed to the high dielectric behavior value. The high dielectric behavior of the PEDOT/GNP nanocomposites could be due to interfacial and space charge polarization at frequency from 100 Hz to 2.3×10^6 Hz. At lower frequencies, the dipole can rapidly respond to follow the field and dipole polarization reached its maximum value, thereby achieving the highest dielectric constant and dielectric loss. At higher frequencies, dipole polarizability was at minimum because the field cannot induce dipole moment and hence the dielectric values were also at minimum [35], [36].

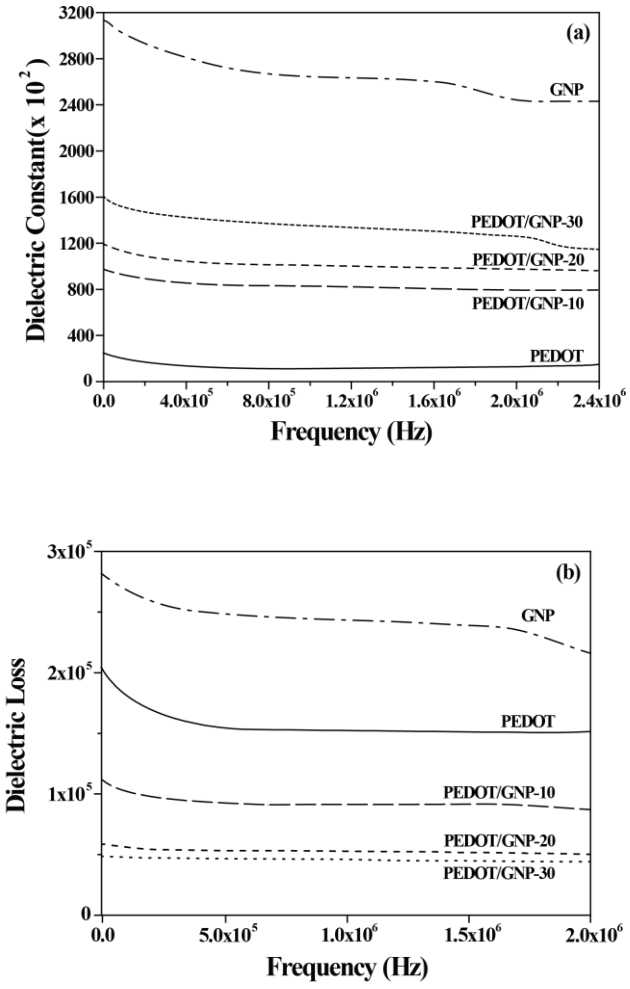

Fig. 8. Frequency-dependent dielectric constants (a) and dielectric losses (b) of PEDOT, GNPs, PEDOT/GNP–10, PEDOT/GNP–20, and PEDOT/GNP–30 within the frequency range of 3.5×10^4 Hz to 2.3×10^6 Hz.

IV. CONCLUSION

New polymer nanocomposites were prepared using PEDOT/GNPs through a simple solid-state polymerization

method. Spectral characterization suggested strong interaction between PEDOT and GNPs in the nanocomposites. Diffraction studies indicated the amorphous nature of the nanocomposites. The frequency-dependent AC electrical conductivity of the prepared nanocomposites was obtained at room temperature within the frequency range of 3.5×10^4 Hz to 2.3×10^6 Hz. The AC electrical conductivities at 3.5×10^4 Hz for PEDOT and GNP were 3.25 and 4.26 S/cm, respectively, whereas the conductivity of the composites increased to 10.76 S/cm. Conductivity increased with increasing frequency and that of the composites significantly increased compared with pure PEDOT and GNPs. PEDOT/GNP nanocomposites present many practical applications, such as in all-organic light-emitting diodes and polymer field-effect transistors. The high electrical conductivity of the nanocomposites may be utilized to fabricate multifunctional materials in bulk for future technological applications. The high dielectric behavior values of the novel polymer nanocomposites further revealed the capacity of these composites to store electric potential energy under an AC field.

ACKNOWLEDGMENT

This research was supported by the National Research Foundation of Korea and funded by the Ministry of Education, Science, and Technology (2013-R1A1A2A100062399).

REFERENCES

[1] Y. Park, D. S. Shin, S. H. Woo, N. S. Choi, K. H. Shin, S. M. Oh, K. T. Lee, and S. Y. Hong, Sodium terephthalate as an organic anode material for sodium ion batteries. *Adv. Mater.*, **24**, 3562-3567 (2012).

[2] S. Renault, D. Brandell, T. Gustafsson, and K. Edström, Improving the electrochemical performance of organic Li-ion battery electrodes. *Chem. Commun.*, **49**, 1945-1947 (2013).

[3] G. A. Snook, P. Kao, and A. S. Best, Conducting-polymer-based supercapacitor devices and electrodes, *J. Power Sources*, **196(1)**, 1-12 (2011).

[4] A. Mihranyan, M. Esmaeili, A. Razaq, D. Alexeichik, and T. Lindström, Influence of the nanocellulose raw material characteristics on the electrochemical and mechanical properties of conductive paper electrodes, *J. Mater. Sci.*, **47**, 4463-4472 (2012).

[5] L. Nyholm, G. Nyström, A. Mihranyan, and M. Strømme, Toward flexible and paper-based energy storage devices. *Adv. Mater.*, **23(33)**, 3751-3769 (2011).

[6] H. S. Nalwa, *Handbook of Organic Conductive Molecules and Polymers*, John Wiley and Sons: New York, Vol. 2, 1997.

[7] D. Fichou, *Handbook of Oligo- and Polythiophenes*, Wiley-VCH: Weinheim Germany, 1999.

[8] T. A. Skotheim, *Handbook of Conducting Polymers*, 3rd edition, J. Reynolds CRC, Boca Raton, FL, 2007.

[9] C. Carlberg, X.Chen and I. Olle, Ionic Transport and Electronic Structure in Poly(3,4-ethylenedioxythiophene). *Solid State Ionics*, **85**, 73-78 (1996).

[10] L. B. Groenendaal, F. Jonas, D.Freitag, H. Pielartzik, and J. R. Reynolds, Poly(3,4-ethylenedioxythiophene) and its derivatives:past,present and future,*Adv. Mater.*, **12(7)**, 481-494 (2000).

[11] L. Groenendaal, G. Zotti, P. –H. Aubert, S. M. Waybright, and J. R. Reynolds, Electrochemisty of Poly(3,4-alkylenedioxythiophene) Derivatives, *Adv. Mater.*, **15**, 855-879 (2003).

[12] G. A. Sotzing, J. R. Reynolds and P. J. Steel, Poly(3,4-ethylenedioxythiophene) (PEDOT) prepared via electrochemical polymerization of EDOT, 2,2'-Bis(3,4-ethylenedioxythiophene) (BiEDOT), and their TMS derivatives, *Adv. Mater.*, **9(10)**, 795-798 (1997).

[13] F. Li , J. Chai, H. Yang, D.Han, and L. Niu, Synthesis of Pt/ionic liquid/graphene nanocomposite and its simultaneous determination of ascorbic acid and dopamine. *Talanta*, **81**, 1063-1068. (2010).

[14] D. Li and R. B. Kaner, Graphene-based Materials, *Science*, **320(5880)**, 1170-1171 (2008).

[15] K. Zhang , L. Mao, L. L. Zhang, X. S. Zhao, and J. Wu, Surfactant-intercalated, chemically reduced graphene oxide for high performance supercapacitor electrodes, J. Mater. *Chem.*, **21**, 7302-7307 (2011).

[16] *T. K. Das and S. Prusty, Graphene-based polymer composites and their applications, Polymer-Plastics Technology and Engineering, 52(4), 319-331 (2013).*

[17] S. Singh, V. K. Srivastava and P. Prakash, Influences of carbon nanofillers on mechanical performance of epoxy resin polymer, *Appl. Nanosci.*, **5**, 305-313 (2015).

[18] M. J. Alien, V. C. Tung, and R. B. Kaner, Honeycomb Carbon: A Review of Graphene, *Chem. Rev.*, 110, 132-145, (2010)

[19]M. D. Stoller, S. Park, Y. Zhu, J. An, and R. S. Ruoff, Graphene-based ultracapacitors, *Nano Letters*, **8(10)**, 3498-502 (2008).

[20] H. He and W. Chen, 3D graphene nanomaterials for binder-free supercapacitors: scientific design for enhanced performance, *Nanoscale*, **7(16)**, 6957-6990 (2015).

[21] K. I. Bolotin, K. J. Sikes, Z. Jiang, M. Klima, G. Fudenberg, J. Hone , P. Kim, and H. L. Stormer, Ultrahigh electron mobility in suspended graphene, *Solid State Commun.*, **146(9-10)**, 351-355 (2008).

[22] A. H. Castro Neto, F. Guinea, N. M. R. Peres, K. S. Novoselov, and A. K. Geim, The electronic properties of graphene, *Rev. Modern Phys.*, **81(1)**, 109-115 (2009).

[23] X. L. Zhao and C. Gao, Progress of Graphene-based Nacre-mimetic Layered Materials, *Acta Polymerica Sinica*, **10**, 1301-1313 (2014).

[24] Y. Q. Li, R. Umer, Y. A. Samad, L. X. Zheng, and K. Liao, The effect of the ultrasonication pre-treatment of graphene oxide (GO) on the mechanical properties of GO/polyvinyl alcohol composites, *Carbon*, **55**, 321-327 (2013).

[25] S. H. Song, K. H. Park, B. H. Kim, Y. W. Choi, G. H. Jun, D. J. Lee, B. S. Kong, K. W. Paik, and S. W. Jeon, Enhanced Thermal Conductivity of Epoxy-Graphene Composites by Using Non-Oxidized Graphene Flakes With Non-Covalent Functionalization, *Adv. Mater.*, **25 (5)**, 732-737 (2013).

[26] Z. P. Chen, C. Xu, C. Q. Ma, W. C. Ren, and H. M. Cheng, Lightweight and flexible graphene foam composites for high-performance electromagnetic interference shielding, *Adv. Mater.*, **25(9)**, 1296-1300 (2013).

[27] N. Andy, D. Lahiri, and A. Agarwal, Synthesis and properties of bulk graphene nanoplatelets consolidated by spark plasma sintering, *Carbon*, **50(11)**, 4068-4077 (2012).

[28] W. Choi, I. Lahiri, R. Seelaboyina, and Y. S. Kang, Synthesis of Graphene and Its Applications: A Review, *Critical Reviews in Solid State and Materials Science*, **35(1)**, 52-71 (2010).

[29] H. Meng, D. F. Perepichka, M. Bendikov, F. Wudl, G. Z. Pan, W. Yu, W. Dong, and S. Brown, Solid-state synthesis of a conducting polythiophene via an unprecendented heterocyclic coupling reaction, J. Am. Chem. Soc., **125(49)**, 15151-15162 (2003).

[30] S. Selvaganesh, T. S. Vinod, J. Mathiyarasu, K. L. N. Phani, and V. Yegnaraman, Chemical Synthesis of PEDOT-Au Nanocomposite, *Nanoscale Res. Lett.*, **2 (11)**, 546-549 (2007).

[31] W. C. William, J. Trava˘s-Sejdi´c, P. C. Ralph, and G. A. Bowmaker, Spectroscopic and conductivity studies of doping in chemically synthesized Poly(3,4-ethylenedioxythiophene) *Synth. Met.*, **155(1)**, 80-88 (2005).

[32] T. Abdiryim, A. Ali, R. Jamal, Y. Osman, and Y. Zhang, A facile solid-state heating method for preparation of poly(3,4-ethelenedioxythiophene)/Zno nanocompositeand photocatalytic activity, *Nanoscale Res. Lett.*, **9(1)**, 89-97 (2014).

[33] C. Basavaraja, W. J. Kim, D. G. Kim, and D. S. Huh, Microwave absorption studies of polyaniline nanocomposites encapsulating gold nanoparticles on the surface of reduced graphene oxide in the presence of 2-naphthalene sulfonic acid, *Colloid Polym. Sci.*, **290**, 829-838 (2012).

[34] Joint Committee on Powder Diffraction Standards, Diffraction data file: JCPDS International Center for Diffraction Data: Swarthmore, PA 1991

[35] S. M. Reda and A. M. Al-Ghannam, Synthesis and Electrical Properties of Polyaniline Composite with Silver Nanoparticles, Adv. Mater. Phys. Chem., **2**, 75-81 (2012).

[36] N. N. Mallikarjuna, S. K. Manohar, P. V. Kulkarni, A. Venkataraman, and T. M. Aminabhavi, Novel high dielectric constant nanocomposites of polyaniline dispersed with γ-Fe_2O_3 nanoparticles, *J. Appl. Polym. Sci.*, **97(5)**, 1868-1874 (2005).

Chitragara Basavaraja has been dedicated to the interdisciplinary research on conducting polymers, nano science and nanotechnology. Recent research includes the studies in nano-scale fabrication and assembly, materials characterization, and nanoscale photocatalysis, etc.

Ju Yeon Park is a MSc course student working on the conducting polymer composites and fabrication of honeycomb-patterned films.

Do Sung Huh is a professor in the department of Chemistry and Nanoscience and Engineering who is interesting nanoscience and nanotechnology including biomimetic materials. He has published over than 80 SCI paper.